Patterning techniques

Molecular Printboards on Silicon Oxide: Lithographic Patterning of Cyclodextrin Monolayers with Multivalent, Fluorescent Guest Molecules**

Alart Mulder, Steffen Onclin, Mária Péter, Jacob P. Hoogenboom, Hans Beijleveld, Jurjen ter Maat, María F. García-Parajó, Bart Jan Ravoo, Jurriaan Huskens, Niek F. van Hulst,* and David N. Reinhoudt**

***T**hree compounds bearing multiple adamantyl guest moieties and a fluorescent dye have been synthesized for the supramolecular patterning of β-cyclodextrin (CD) host monolayers on silicon oxide using microcontact printing and dip-pen nanolithography. Patterns created on monolayers on glass were viewed by laser scanning confocal microscopy. Semi-quantitative analysis of the patterns showed that with microcontact printing approximately a single monolayer of guest molecules is transferred. Exposure to different rinsing procedures showed the stability of the patterns to be governed by specific supramolecular multivalent interactions. Patterns of the guest molecules created at CD monolayers were stable towards thorough rinsing with water, whereas similar patterns created on poly(ethylene glycol) (PEG) reference monolayers were instantly removed. The patterns on CD monolayers displayed long-term stability when stored under N_2, whereas patterns at PEG monolayers faded within a few weeks due to the diffusion of fluorescent molecules across the surface. Assemblies at CD monolayers could be mostly removed by rinsing with a concentrated CD solution, demonstrating the reversibility of the methodology. Patterns consisting of different guest molecules were produced by microcontact printing of one guest molecule and specific adsorption of a second guest molecule from solution to non-contacted areas, giving well-defined alternating assemblies. Fluorescent features of sub-micrometer dimensions were written using supramolecular dip-pen nanolithography.*

Keywords:
- cyclodextrin
- dip-pen nanolithography
- laser spectroscopy
- microcontact printing
- monolayers

[*] Dr. A. Mulder,[+] Dr. S. Onclin,[+] Dr. M. Péter, H. Beijleveld, J. ter Maat, Dr. B. J. Ravoo, Dr. J. Huskens, Prof. Dr. D. N. Reinhoudt
Laboratory of Supramolecular Chemistry and Technology
MESA+ Institute for Nanotechnology
University of Twente
P. O. Box 217, 7500 AE Enschede (The Netherlands)
Fax: (+31) 53-4894645
E-mail: j.huskens@utwente.nl
d.n.reinhoudt@utwente.nl

Dr. J. P. Hoogenboom, Dr. M. F. García-Parajó, Prof. Dr. N. F. van Hulst
Applied Optics Groups
MESA+ Institute for Nanotechnology
University of Twente
P. O. Box 217, 7500 AE Enschede (The Netherlands)
Fax: (+31) 53-4893172
E-mail: n.f.vanhulst@tnw.utwente.nl

[+] Both authors contributed equally to this work.

[**] This research is supported by the Council for Chemical Sciences of the Netherlands Organization for Scientific Research (CW-NWO) (A.M.: CW-programmasubsidie 700.98.305), the MESA MICS program (S.O.), the VW-Stiftung (J.P.H.) and the Technology Foundation STW, applied science division of NWO and the technology program of the Ministry of Economic Affairs (M.P.: Simon Stevin Award to D.N.R., project number TST4946).

DOI: 10.1002/smll.200400063

NANO MICRO small

1. Introduction

The use of supramolecular interactions for the immobilization of molecules at surfaces has been a relatively unexplored research topic in the field of supramolecular chemistry for many years, and has only recently become a subject of growing interest as the attractive characteristic features associated with this methodology, that is, high specificity, controllable affinity, and reversibility of immobilization become evident.[1–6] Multivalent interactions[7] are especially suitable for application in immobilization schemes.[3–6,8–10] The combination of multiple, intrinsically weak, host–guest interactions can be used to form complexes that are thermodynamically and/or kinetically stable, but that can be dissociated by competition with monovalent host or guest species.[4,7,10,11] The interaction strength of the multivalent interaction can be fine-tuned by controlling 1) the number of host–guest interactions,[4,11] and 2) the strength of the intrinsic interaction.[4,11]

We have used β-cyclodextrin (CD) host–guest interactions for the immobilization of guest molecules, that is, interactions between CD-host self-assembled monolayers (SAMs) and molecules modified with multiple hydrophobic guest moieties. CD SAMs are particularly interesting surfaces for application in supramolecular immobilization schemes, because of the dense hexagonal packing of the monolayers[12,13] and the broad range of affinities of CD for different hydrophobic guest moieties.[14] Over the last five years, we have studied the interaction of various guest molecules with CD monolayers, both mono-[15–17] and multivalent.[4,11,18–20] In a recent communication we have shown that these CD monolayers can be used as "molecular printboards"[4] that can be supramolecularly patterned using lithographic techniques such as microcontact printing (μCP) and dip-pen nanolithography (DPN).[19] Different molecular architectures suitably modified with hydrophobic adamantyl groups were applied to pattern CD SAMs on gold and CD monolayers on silicon oxide (SiO_2).[19] This methodology enabled the creation of supramolecular patterns with sub-100 nm resolution that were stable towards aqueous rinsing procedures, but could be mostly removed by rinsing with concentrated CD solutions.[19] The advantage of these supramolecular lithographic patterning schemes over lithographic schemes based on physisorption[21–23] or covalent chemistry[24] lies in the specificity and directionality of the supramolecular interaction and the tunability of the type and number of host–guest interactions. Compared to traditional lithographic techniques, such as the patterning of gold substrates with thiols,[25,26] supramolecular lithography offers the possibility to erase the created patterns.[19]

The CD monolayers on SiO_2 have been developed as an alternative molecular printboard that is, in contrast to the CD SAMs on gold, compatible with fluorescence imaging.[27,28] Apart from eliminating fluorescence quenching, which is a serious problem when using SAMs on gold, the SiO_2 substrates enable the use of transmission optics such as laser scanning confocal microscopy (LSCM) and near-field scanning optical microscopy (NSOM), which are powerful and sensitive microscopic techniques that allow the study of molecules at monolayers.[29–31] As with AFM, it is possible to image (sub)micrometer patterns with NSOM and LSCM, as well as to perform single-molecule studies.[29,30] Additionally, NSOM and LSCM enable online monitoring of processes occurring at the surface and quantification of the (relative) amounts of molecules present at the surface.[31] Furthermore, LSCM allows a straightforward discrimination between different types of molecules present at the surfaces, provided these are suitably modified with fluorescent dyes.[32]

For this paper the combination of molecular printboards on SiO_2 and LSCM has been applied to get a better, more quantitative, understanding of supramolecular lithography in terms of, for example, ink transfer and pattern stability, and to further expand the versatility of the concept of molecular printboards by generating defined patterns consisting of multiple, different guest molecules.

2. Results and Discussion

2.1. Monolayers on SiO_2

Figure 1 depicts the structures of the monolayers employed in this study. The synthesis of the CD monolayers on SiO_2 (Figure 1, left) has been reported previously.[20] Considering molecular packing and host–guest binding properties, these CD monolayers on SiO_2 are comparable to the CD SAMs on gold. XPS analysis indicated that the CDs are rigidly anchored at the SiO_2 surface with an average of three covalent bonds per CD ($x = 3$ in Figure 1), which renders the secondary side of the CDs to be exposed to solution. For the CD monolayers on SiO_2, a surface density of one CD cavity per 2.3 nm^2 was calculated,[20] which was only marginally less than the 2.1 nm^2 determined for the CD SAMs on gold with AFM.[13] Furthermore, the interaction of a bis(adamantyl)-functionalized guest molecule with the CD

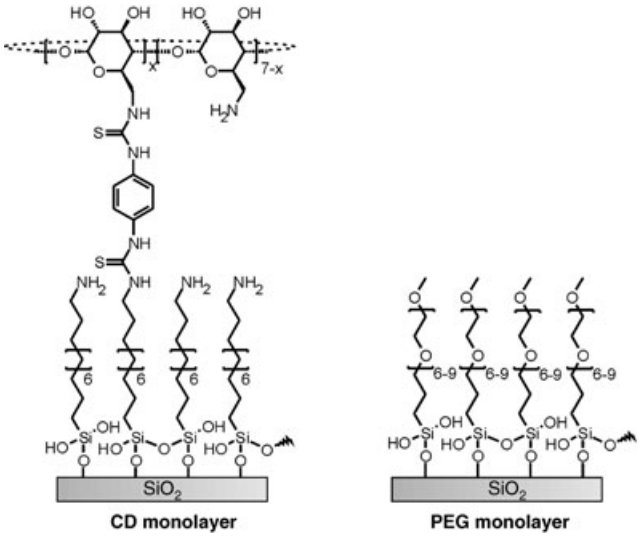

Figure 1. Structures of the CD and PEG monolayers on SiO_2.

monolayers at SiO_2 gave a binding constant of $\approx 10^{10}\,M^{-1}$,[20] which was similar to that found for the interaction of the bis(adamantyl)-calix[4]arene with CD SAMs on gold,[18] which indicates that multivalent guest molecules interact with both CD monolayers in a similar fashion.

Monolayers of poly(ethylene glycol) (PEG) chains (Figure 1, right) were used as reference layers. PEG monolayers are known to resist nonspecific adsorption,[33,34] and were therefore expected to have a low affinity for hydrophobic guest molecules. The PEG monolayers on SiO_2 were prepared using a literature procedure by Papra et al.[35]

2.2 Design and Synthesis of the Multivalent Fluorescently Labeled Guests

Three fluorescent adamantyl-functionalized molecules, **1**–**3**, were synthesized for supramolecular patterning of CD monolayers on SiO_2 (see Scheme 1). The design of **1**–**3** was based on molecules that previously have been shown to strongly interact with CD monolayers on gold. The structure of **1** is based on a second-generation poly(propylene imine) (PPI) dendritic wedge with four adamantyl groups at its periphery. Structurally, **1** is similar to adamantyl-functionalized PPI dendrimers, which have been shown to interact via specific adamantyl–CD interactions with CD SAMs on gold.[4] From these studies it was shown that a second-generation PPI wedge was required to allow a divalent interaction with the CD SAMs on gold, since the spacing of the CD cavities on gold does not allow two adamantyl moieties of a single branch to simultaneously bind to the SAM. As the packing of the CDs on SiO_2 is similar to the packing on gold (see above), a second-generation wedge was synthesized for the interaction with the CD monolayers on SiO_2. A lissamine moiety at the focal point of the dendritic wedge **1** was used as a fluorescent label.

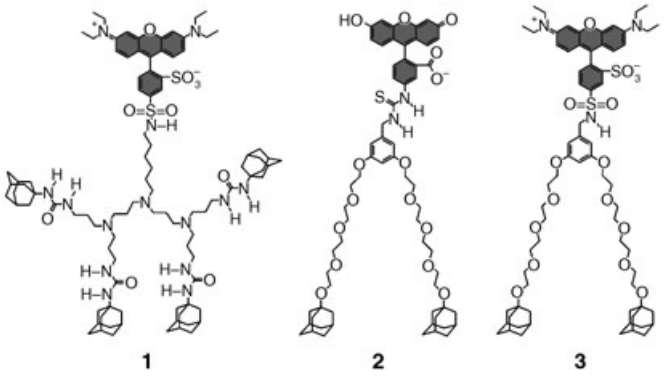

Scheme 1. Fluorescent adamantyl-terminated dendritic wedges used for interaction with the CD monolayers on SiO_2.

For molecules **2** and **3**, long, flexible tetraethylene glycol spacers were employed to ensure a divalent interaction with the CDs at the SiO_2 surface. This strategy has been used previously by our group for interaction of bis-[18,19] and tetra(adamantyl)-calix[4]arenes[36] with CD SAMs on gold. In **2** and **3**, a phenyl unit was used to couple a fluorescent dye to two adamantyl moieties; **2** bears the green fluorescent fluorescein dye, whereas the red fluorescent lissamine dye is used for labeling in **3**.

The synthesis route for the fluorescent adamantyl-terminated PPI wedge **1** is outlined in Scheme 2. The synthesis starts from *N*-Boc-1,6-diaminohexane and the construction of the dendritic wedge is analogous to the synthesis of PPI dendrimers.[37] *N*-Boc-1,6-diaminohexane was dispersed in water and treated with acrylonitrile to form dinitrile **4** via a Michael addition. Reduction of the nitrile groups of **4** with Raney cobalt and hydrogen in methanol/ammonia/water at 8 bar and room temperature gave diamine **5**. This diamine was cyanoethylated according to the procedure outlined

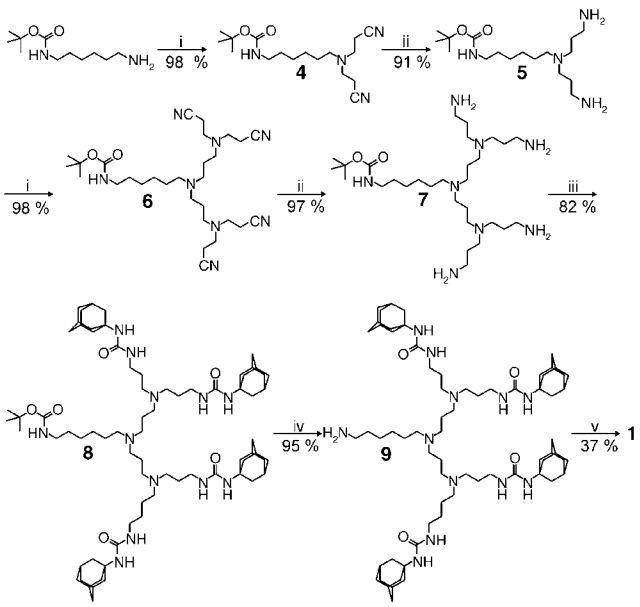

Scheme 2. Synthesis route towards fluorescent PPI wedge **1**: i) Acrylonitrile, H_2O, 100 °C, overnight; ii) Raney Co, 8 bar H_2, NH_3 (aq), RT, 5 h; iii) 1-adamantyl isocyanate, $CHCl_3$, RT, overnight; iv) TFA, CH_2Cl_2, 0 °C, 30 min; v) lissamine sulfonyl chloride (mixture of isomers), DIPEA, CH_2Cl_2, RT, overnight.

NANO MICRO small

above to form the second-generation tetranitrile wedge **6**, which was subsequently reduced to tetraamine **7**. The free amino groups of **7** were reacted with 1-adamantyl isocyanate to give the tetraadamantyl-functionalized Boc-protected amine wedge **8**. The Boc group was removed using TFA, and the resulting free amine **9** was reacted with lissamine sulfonyl chloride to give **1**.

Scheme 3 depicts the synthesis routes for **2** and **3**. Nucleophilic substitution on 1-bromo-adamantane with tetraethylene glycol in the presence of triethylamine gave the monoadamantyl-functionalized tetraethylene glycol **10**.[18] Subsequent conversion of the remaining hydroxyl functionality to

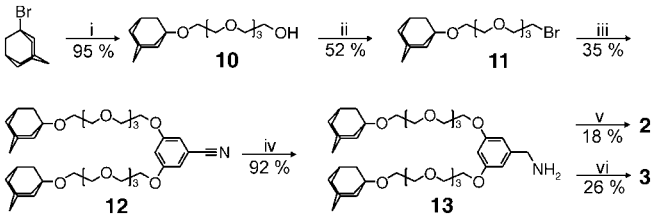

Scheme 3. Synthesis route towards the fluorescent adamantyl-functionalized guests **2** and **3**: i) Et_3N, tetraethylene glycol, 180 °C, overnight; ii) PBr_3, toluene, RT, overnight; iii) 3,5-dihydroxybenzonitrile, K_2CO_3, [18]crown-6, acetone, reflux, 72 h; iv) Raney Co, 6 M NH_3 in ethanol, 5 bar H_2, RT, overnight; v) fluorescein isothiocyanate, DIPEA, MeOH, CH_2Cl_2, RT, overnight; vi) lissamine sulfonyl chloride (mixture of isomers), DIPEA, acetonitrile, RT, overnight.

a bromide, using PBr_3 in toluene, gave bromide **11**. Reaction of **11** with 3,5-dihydroxybenzonitrile under conditions used by Hawker and Fréchet,[38] that is, acetone, K_2CO_3, and [18]crown-6, gave the divalent wedge **12**. The nitrile functionality of **12** was converted to an amine by hydrogenation with 5 bar H_2 to yield **13**, which was used as a precursor for the fluorescent wedges **2** and **3**.[39] Fluorescein-functionalized wedge **2** was obtained by reaction of **13** with fluorescein isothiocyanate. Lissamine-functionalized wedge **3** was formed by reaction of **13** with lissamine sulfonyl chloride.

Figure 2 depicts the combined and normalized excitation and emission spectra of aqueous solutions of **2** (left) and **3** (right). Both emission and excitation spectra are typical of the fluorescent dyes incorporated in the molecules. Fluorescein-functionalized **2** showed an excitation maximum in aqueous solution at 493 nm and an emission maximum in the green region at 521 nm. Lissamine-functionalized **3** showed an excitation maximum in aqueous solution at 569 nm with an emission maximum in the red region at 589 nm. Excitation and emission spectra recorded for **1** were similar to those of **3**.

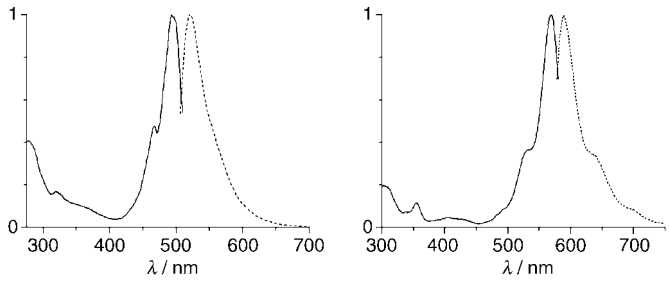

Figure 2. Normalized excitation (----) and emission (——) spectra (1 μM in water) of fluorescein-functionalized wedge **2** (left) and lissamine-functionalized wedge **3** (right).

2.3. Supramolecular Microcontact Printing

Microcontact printing (μCP) was applied to produce μm-scale patterns of assemblies on the CD monolayers on SiO_2. Figure 3 depicts LSCM images of patterns of **1** printed on two differently modified SiO_2 substrates. To allow for fluorescence imaging, μCP of **1** was performed on functionalized glass slides, that is, glass slides functionalized with a CD monolayer (top three images of Figure 3) and, as a reference experiment, glass slides with a PEG monolayer (bottom two images of Figure 3). Printing of **1** was performed from aqueous solution as the per-CD complex of **1** (10 μM **1** in 10 mM CD), using oxidized PDMS stamps (10 μm features spaced by 5 μm). The per-CD complex of **1** was used to achieve sufficiently concentrated solutions of **1** for printing. The free ligand **1** was only scarcely water soluble. Complexation of the hydrophobic adamantyl moieties by solubilizing **1** in 10 mM CD solutions improved the water solubility of **1** to the high μM range. The PDMS stamps were mildly oxidized using UV/ozone to ensure a good adhesion of the aqueous ink solution to the stamp. As is evident from Figure 3, ink transfer is achieved both on the CD and PEG monolayers, and in both cases a faithful reproduction of the stamp features are obtained. Thorough rinsing of the substrates with copious amounts of 10 mM phosphate buffer led to complete removal of the patterns on the PEG monolayers, whereas this rinsing procedure hardly affected the patterns printed on the CD substrates. Only rinsing with 10 mM

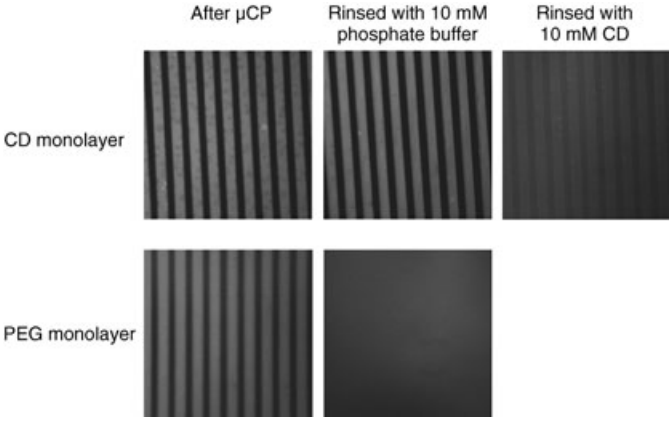

Figure 3. Confocal microscopy images (150 × 150 μm^2) after μCP of the per-CD complex of **1** on CD (top) and PEG (bottom) monolayers on SiO_2. Images shown after printing from left to right: without rinsing; after rinsing with 200 mL of 10 mM phosphate buffer (pH 6.8); after rinsing with 200 mL of a 10 mM aqueous CD solution. Images obtained after printing and subsequent rinsing procedures were captured at identical confocal microscope settings.

CD led to significant reduction of the fluorescence intensity on the latter substrates.

These results indicate that multivalent, specific interactions between **1** and the CD monolayer are responsible for the observed stability of the patterns. Furthermore, they illustrate that per-CD-complexed molecules are well suited for use in printing experiments. Apparently, the concentration of CD cavities at the surface is sufficiently high to compete with the CD molecules that are transferred together with **1** upon printing. These findings are in line with the theoretical model presented previously,[11,18] and corroborate the assumption that the CD cavities are closely packed on the SiO_2 substrates, which gives rise to a considerable effective surface CD concentration that is experienced by the guest molecules.

Similarly, μCP experiments were performed with fluorescent wedges **2** and **3**. The confocal microscopy images of the patterns on CD monolayers are depicted in Figure 4.

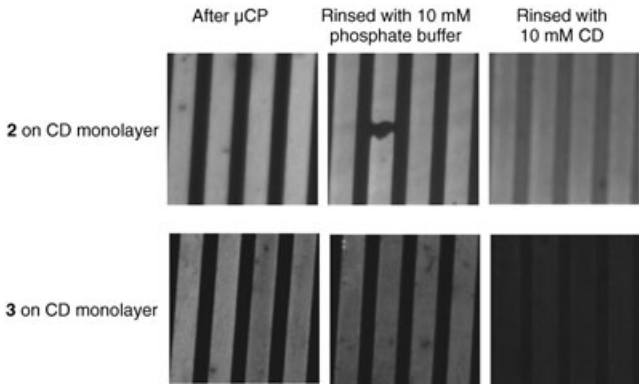

Figure 4. Confocal microscopy images (60 × 60 μm²) after μCP of fluorescent dendritic wedges **2** (top) and **3** (bottom) on a CD monolayer on SiO_2. Images shown after printing, from left to right: without rinsing, after rinsing with 200 mL of 10 mM phosphate buffer (pH 6.8); after rinsing with 200 mL of a 10 mM aqueous CD solution. Images obtained after printing and subsequent rinsing procedures were captured at identical confocal microscope settings.

The top row shows patterns of fluorescein-derivatized **2**, the bottom row the patterns of lissamine-labeled **3**. **2** was moderately water soluble at high pH values, and an aqueous solution containing 0.1 mM of the free ligand **2** was used for printing. Since **3** is poorly water soluble, it was printed as the per-CD complex (10 μM **3** in 10 mM CD). Patterns produced with both wedges showed similar stabilities towards rinsing with aqueous solutions as for **1**, that is, patterns printed on PEG monolayers were completely removed upon rinsing with aqueous solutions (data not shown), whereas patterns on the CD monolayers were stable towards rinsing with water and 10 mM phosphate buffer. These patterns could only be partially removed by rinsing the substrates with concentrated CD solutions.

Comparison of the sets of LSCM images displayed in Figure 3 and Figure 4 indicates that the stability of the patterns of tetravalent guest **1** on the CD monolayers is similar to that of the divalent guests **2** and **3**. Recently, we have shown that the divalent wedge **2** interacts strongly with CD monolayers on SiO_2.[20] By means of desorption experiments it was shown that these molecules bind to the CD monolayers on SiO_2 via a divalent interaction.[20] This suggests that all three guest molecules **1**–**3** bind to the CD monolayer via a divalent interaction.[40] As mentioned above, a divalent interaction between **1** and the CD monolayer was expected and these observations are in line with the results obtained for the interactions between adamantyl-terminated dendrimers and CD SAMs on gold.[4,11] Even though complete desorption of the fluorescent wedges by competitive rinsing has not been proven here, this can probably be achieved by using larger volumes, preferably in a flow-cell setup to diminish rebinding, and has been shown to be successful for a bis(adamantyl)-calix[4]arene.[18] An alternative for more efficient desorption is to use electroactive guest motifs which allow electrochemical desorption.[19,41]

One of the advantages of LSCM is that, in contrast to AFM, it allows a direct semi-quantitative analysis of the amount of fluorescent material that is transferred to the substrate upon μCP, and of that which is present at the substrates after the rinsing procedures, thus offering a measure to investigate pattern stability and ink transfer during μCP. Previously, we have shown with XPS that supramolecular μCP of a 0.1 mM solution of the bis(adamantyl)-calix[4]arene on CD SAMs on gold appears to result in multilayer formation on the SAM.[19] This multilayer could be reduced to approximately a monolayer of guest molecules by rinsing with a phosphate buffer. The transfer of multilayers by μCP is not uncommon. Although μCP of alkanethiols on gold has been shown to result in rapid and clean formation of a monolayer,[42,43] μCP generally leads to the formation of submonolayers or multilayers, depending mainly on the ink concentration and applied contact time.[44–46] Figure 5 shows that this is not the case for μCP of fluorescent wedge **3** (1 μM in 10 mM CD). The left side of Figure 5 depicts an LSCM image of the edge of an area where the substrate (a glass slide modified with a CD monolayer) was exposed to a droplet of an aqueous solution of **3** (1 μM in 10 mM CD). The image was taken after 5 min of adsorption and rinsing of the substrate with water to remove physisorbed material,

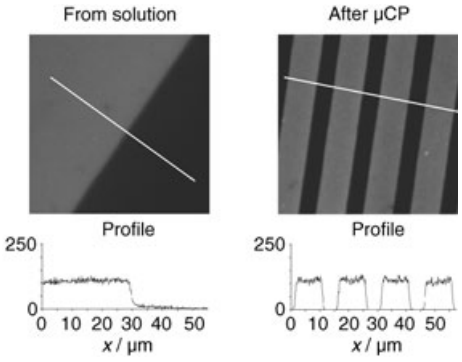

Figure 5. Confocal microscopy images (60 × 60 μm²) and emission intensity graphs of fluorescent dendritic wedge **3** on a CD monolayer on SiO_2. Left: **3** adsorbed from solution after rinsing the sample with 10 mM phosphate buffer (pH 6.8). Right: **3** directly after μCP, without rinsing the sample. Images were obtained at identical confocal microscopy settings.

NANO MICRO small

presumably leaving a single layer of guest molecules on the CD printboard.[47] The right side depicts the LSCM image of a pattern of **3** generated by μCP from the same solution. The image was obtained directly after μCP without rinsing the sample and using the exact same settings on the confocal microscope as the image on the left. Comparison of the fluorescence intensity profiles indicates that a similar amount of fluorescent molecules is present on both surfaces, which demonstrates that printing of **3** from a 1 μM solution results in the transfer of approximately one monolayer. Profile analysis of these patterns with AFM was not performed as no patterns were observed in the height images. The transfer of approximately a monolayer suggests that supramolecular μCP ink transfer is also concentration dependent. As mentioned above, μCP of a 0.1 mM solution of a bis(adamantyl)-calix[4]arene on CD SAMs led to multilayer formation, resulting in a monolayer after rinsing.[19] Also, μCP of dilute (1 μM) solutions of wedges **1** and **2** led to the transfer of approximately a monolayer.

To assess the long-term stability of the supramolecular patterns, substrates that had been microcontact printed with **3** were stored in the dark in a nitrogen atmosphere and imaged after certain time intervals. An identical experiment was also performed on a PEG reference monolayer to evaluate the significance of specific interactions for long-time stability. The LSCM images and corresponding fluorescence intensity profiles obtained directly after printing are depicted in Figure 6 (left). Subsequently, the substrates were stored in the dark and imaged again after one week (Figure 6, middle), and after six weeks (Figure 6, right). Comparison of the LSCM images and profiles shown in Figure 6 indicates that stable patterns are formed on the CD monolayer, that is, there was no sign of pattern degradation, even after six weeks of storage. In contrast, patterns

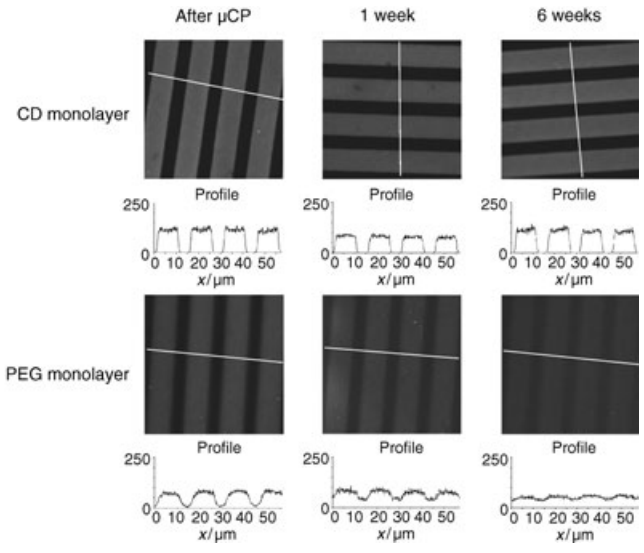

Figure 6. Confocal microscopy images (60 × 60 μm²) of a CD monolayer (top three images) and a PEG monolayer (bottom three images) patterned with **3** without rinsing. Images were taken: directly after printing (left), and after storing under dark conditions for one week (middle) and six weeks (right). All images were captured at identical confocal microscope settings.

prepared on a reference PEG monolayer gradually started to fade with time, thus suggesting that CD–adamantyl interactions are required to keep the printed molecules in place. The principal factors involved in binding guest molecules by CDs are believed to be van der Waals and hydrophobic interactions.[48] Hydrophobic interactions require water to be present at the CD interface. As these monolayers are quite hydrophilic it is likely that water will still be present, even under "dry" conditions, which could account for the observed stability of microcontact-printed patterns under these conditions.

The observation of sharp and stable edges after six weeks of storage under dark conditions corroborates our assumption that approximately one monolayer of guest molecules is transferred during printing under these conditions, as multilayers of **3** would be susceptible to the spreading behavior observed for the PEG monolayers. The fact that this was not observed suggests that all guest molecules present at the surface interact with the CD monolayer.

As mentioned above, an additional advantage of LSCM over AFM is that it allows an easy discrimination between different dye molecules present at the surface.[32] An example of how LSCM enables the straightforward discrimination between different species immobilized at the molecular printboard is shown in Figure 7, which depicts the LSCM

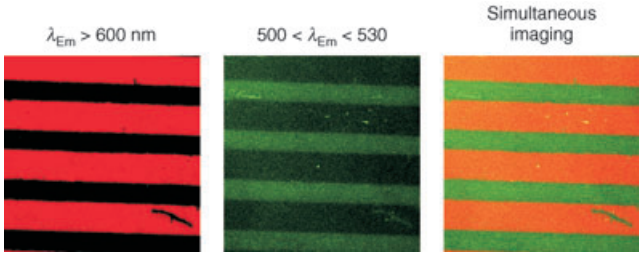

Figure 7. Confocal microscopy images (60 × 60 μm²) taken at different emission wavelengths of a CD monolayer on a glass slide patterned with **1** by μCP and subsequently immersed in an aqueous solution of **2**. The substrate was simultaneously excited at 488 and 543 nm and images were recorded by measuring the emission above 600 nm (left) and between 500 and 530 nm (center). The combined image is shown at the right. A deeper red LSCM output color was selected to resemble the lissamine dye in order to have two strongly contrasting colors.

images acquired at different emission wavelengths. The CD monolayer on glass was patterned by μCP with **1** (according to the procedure described above), rinsed with a 10 mM phosphate buffer, and subsequently immersed in an aqueous solution of **2** (0.1 mM). The LSCM emission image recorded above 600 nm is dominated by the emission of the printed lines of **1** (Figure 7, left). The lissamine dye of **1** has a strong emission above 600 nm, whereas the emission of the fluorescein-functionalized **2** is very limited at these wavelengths (see Figure 2). As is evident from the LSCM emission image recorded between 500 and 530 nm, the range of wavelengths at which fluorescein strongly emits (Figure 7, center), **2** was specifically adsorbed at the vacant CD cavities that had not been in contact with the PDMS stamp. The

sharp contrast in the patterns, as seen in the LSCM images of the individual guest molecules (Figure 7, left and middle), suggests that there is only limited replacement of **1** by **2**.

2.4. Supramolecular Dip-Pen Nanolithography

Dip-pen nanolithography (DPN) is a very powerful technique to write features at the sub-100-nm scale .[26] Here we used DPN to write fluorescent patterns on the CD monolayers. To reduce the activation energy required for molecular transport from the AFM tip to surface, gold-coated Si_3N_4 tips were covered with a (1-mercapto-11-undecyl)tri(ethylene glycol) SAM.[49,50] Tips were soaked in a 0.1 mM ethanolic solution of **3** for ≈5 min before being dried in air. It is known that relative humidity is an important factor in the transport of high-molecular-weight molecules from tip to surface.[51] Therefore, the DPN experiments were carried out at a relatively high humidity, typically between 45 and 55%, and at a temperature of 29°C. Figure 8 depicts a typical pattern of **3** produced by DPN. After inking of the AFM tip the pattern was scanned across the surface with a scan velocity of ≈10 μm s^{-1} to produce a cross with lines 10 μm long and 160 nm wide. Each line was scanned for 10 min. After scanning, the glass substrate was imaged by LSCM (Figure 8, left) and thereafter the same substrate was inspected by lateral force microscopy (LFM; Figure 8, right).

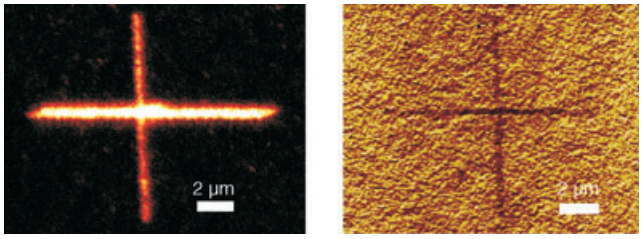

Figure 8. Confocal microscopy (left) and lateral force microscopy (right) images (25 × 21 μm^2; LSCM: 512 × 512 pixels) of a pattern of **3** generated by dip-pen nanolithography on a CD monolayer on a SiO_2 glass slide. Friction forces (a.u.) increase from dark to bright contrast in the image on the right.

Both images clearly show that guest molecules were transferred to the surface.[52] A comparison of the images shown in Figure 8 indicates that LSCM provides a better quantitative analysis of the generated patterns. The LSCM image clearly shows that the produced cross was made up of two lines with different widths and intensities, whereas in the image obtained by LFM this is less apparent. The observed line widths by LSCM are 475 nm for the horizontal line and 400 nm for the vertical line, but contain the convolution of the point-spread function. Analysis of the LFM friction image gave mean line widths of approximately 400 nm for both lines. The deviation from the programmed AFM line width (160 nm) could be explained by a drift in the AFM scanner or by deposition of more than a monolayer of guest molecules. As the horizontal line has the shape of a diamond, it suggests a drift due to scanning. The higher fluorescence intensity found for the horizontal line is indicative of deposition of a relatively higher number of guest molecules. Apparently, the transfer of ink took place mainly during the first 10 min of scanning, leaving less ink to write the second line.

To gain an insight into the amount of molecules transferred during a DPN experiment and to study the stability of the generated patterns, rinsing procedures were applied. Patterns were generated by DPN and directly imaged by LSCM, after which the substrate was dismounted from the confocal microscope and rinsed with copious amounts of water, remounted, and imaged again. Figure 9 depicts the LSCM images (top) of a pattern of **1** generated by DPN from an aqueous solution of **1** (10 μM **1** in 10 mM CD). LSCM images of the patterns were taken directly after the DPN experiment (top left) and after rinsing the sample with 200 mL of a 10 mM aqueous phosphate buffer (top right). The bottom graphs in Figure 9 depict the relative (bottom left) and normalized (bottom right) emission intensity line scans of the patterns before and after the rinsing procedure; the colored markers in the LSCM images depict the positions of the line scans.

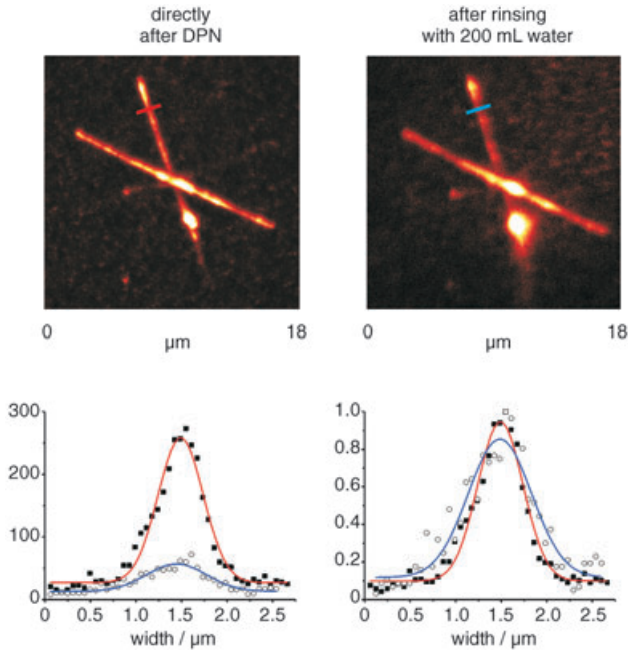

Figure 9. Confocal microscopy images (32 × 29 μm^2; 512 × 512 pixels) of a pattern of **1** produced by DPN on a CD monolayer on glass; directly after writing (top left) and the same pattern after rinsing with 200 mL water (top right). The bottom graphs show the relative (bottom left) and normalized (bottom right) emission intensity line scans (markers) and Gaussian fits (solid lines) for the cross sections of the fluorescent lines before (■) and after (○) rinsing. The positions of the line scans are marked in the top LSCM graphs by the colored bars.

As can be seen from Figure 9, the pattern is still clearly visible after rinsing, which indicates that the pattern stability

NANO MICRO small

is governed by specific multivalent hydrophobic interactions. The line scans of the fluorescent pattern (relative emission intensities, bottom left graph) show that the fluorescence intensity of the pattern was substantially diminished after rinsing. However, this might be either due to desorption of dye molecules, photobleaching of the lissamine dye, or a combination of the two, and therefore care should be taken with the relative quantification of the dye molecules present at the surface. From the bottom right graph in Figure 9 showing the normalized emission intensities for the same line scans, it was calculated that the width of the fluorescent lines increased by about 30% after rinsing with water. This broadening might indicate that more than a monolayer of **1** was transferred during the DPN experiment, and that part of the excess of **1** was able to interact with the CD surface upon rinsing of the pattern. Alternatively, broadening might also be caused by migration of **1** over the surface, which is promoted by a strong effective concentration (C_{eff}) gradient present at the surface, that is, the value of C_{eff} in the substrate areas where most of the CD cavities are complexed by **1** is substantially lower than that in substrate areas where all CDs are free for complexation. Similar spreading may also occur upon rinsing of the μCP patterns. However, for the μCP patterns, line broadening of this order (10–100 nm) is difficult to visualize.

3. Conclusions

Lithographic techniques such as μCP and DPN can be employed to position guest molecules on preformed monolayers exposing host molecules, which function as molecular printboards. Supramolecular μCP of adamantyl-functionalized molecules on CD monolayers on SiO_2 leads to the formation of patterns that are stable towards thorough aqueous rinsing procedures, but can be mostly removed by rinsing with a concentrated CD solution, which induces competition between binding in solution and at the CD monolayer. Specific host–guest interactions give rise to long-term pattern stability when stored under N_2. Sub-μm scale features can be written using supramolecular DPN.

The results of the patterning experiments on CD monolayers on SiO_2 are comparable to those on CD SAMs on gold reported previously,[19] reflecting the similarity of the two receptor interfaces and the general applicability of the molecular printboard concept. The main advantage of the CD monolayers on SiO_2 over the CD SAMs on gold is the capability of using fluorescence imaging techniques for the visualization of the generated patterns, which is strongly hampered when using gold substrates because of quenching. When using fluorescent guest molecules, these techniques can be used complementary to AFM and TOF-SIMS measurements, which have been employed previously for the characterization of supramolecular patterns on CD SAMs.[19] LSCM provides direct evidence for the transfer of guest molecules to the substrate and enables a better (relative) quantification of the patterns generated. Additionally, LSCM enables the straightforward discrimination between different molecules at the interface, providing a handle to monitor the position of different molecules on a surface. Patterns consisting of multiple, different molecules are readily available by combining μCP with adsorption of guest molecules from solution.

We envision that the combination of LSCM with the molecular printboards allows the detailed study of thermodynamics and kinetics of (multivalent) host–guest interactions at monolayers, either directly by developing fluorescent guest molecules such as those reported in this paper, or indirectly by the use of these fluorescent guests in competition experiments, as well as for single-molecule studies. Furthermore, the combination is considered a powerful tool for following the nanoconstruction of more complex, multicomponent, supramolecular structures at (patterned) surfaces.

4. Experimental Section

Materials and Methods: All chemicals were used as received, unless otherwise stated. Solvents were purified according to standard laboratory methods.[53] Thin-layer chromatography was performed on aluminum sheets precoated with silica gel 60 F254 (Merck). Spots of the PPI wedges were visualized by exposure of the TLC plates to iodine and/or bromocresol green. Chromatographic separations were performed on silica gel 60 (Merck, 0.040–0.063 mm, 230–240 mesh). FAB mass spectra were recorded with a Finnigan MAT90 spectrometer with *m*-nitrobenzyl alcohol used as a matrix. MALDI-TOF mass spectra were recorded using a PerSpective Biosystems Voyager-DE-RP MALDI-TOF mass spectrometer using dihydroxybenzoic acid as a matrix. NMR spectra were recorded at 25 °C using a Varian Inova 300 spectrometer. ^{1}H NMR chemical shifts (300 MHz) are given relative to residual $CHCl_3$ (7.25 ppm) or CHD_2OD (3.35 ppm). ^{13}C NMR chemical shifts (75 MHz) are given relative to $CDCl_3$ (77.0 ppm) or to CD_3OD (49.3 ppm).

Substrate preparation: CD monolayers on silicon oxide were prepared as described in Ref. [20]. The PEG monolayers were made by exposure of a cleaned and activated SiO_2 substrate to a commercially available mixture of 2-[methoxyoligo(ethylenoxy)-propyl]trimethoxysilane (6–9 ethylene glycol units per molecule), according to a literature procedure.[35]

4: *N*-Boc-1,6-diaminohexane hydrochloride (1.87 g, 8.65 mmol) was washed with 1 M NaOH and dispersed in water (18 mL). To the dispersion was added acrylonitrile (1.45 mL, 21.6 mmol). The mixture was stirred for 30 min at room temperature, and then refluxed overnight. Excess acrylonitrile was azeotropically removed with water under reduced pressure. Dichloromethane was added, and the organic layer was washed with water, dried over $MgSO_4$, and the dichloromethane was removed under reduced pressure to give **4** as a colorless oil (2.72 g, 8.42 mmol; 98%). ^{1}H NMR ($CDCl_3$): $\delta = 4.52$ (s, 1H; NH), 3.07 (q, $J = 6.6$ Hz, 2H; $NHCH_2$), 2.82 (t, $J = 6.8$ Hz, 4H; CH_2CN), 2.49 (t, $J = 7.0$ Hz, 2H; NCH_2), 2.43 (t, $J = 6.8$ Hz, 4H; NCH_2), 1.47–1.27 (m, 8H; $CH_2CH_2CH_2CH_2$), 1.41 ppm (s, 9H; CH_3); ^{13}C NMR ($CDCl_3$): $\delta = 155.5$, 118.1, 78.5, 52.9, 49.2, 39.9, 29.5, 27.9, 26.8, 26.2, 26.1, 16.5 ppm; MS (FAB): m/z calcd for $[M+H]^+$: 323.2; found: 323.2.

5: An excess of ammonia in water was added to a nitrogen-flushed solution of dinitrile wedge **4** (0.30 g, 0.93 mmol) in methanol. Cr-promoted Raney cobalt (Grace 2724) was added and the mixture was flushed with hydrogen and subsequently hydrogenated at 8 bar H_2 in an autoclave for 5 h at room temperature. Hydrogen was removed by purging with nitrogen and the Raney cobalt was removed over a hyflo filter. The solvent was removed under reduced pressure to give **5** as a colorless oil (0.28 g, 0.85 mmol; 91%). ^{1}H NMR (CD_3OD): $\delta = 3.06$ (t, $J = 7.0$ Hz, 2H; $NHCH_2$), 2.70 (t, $J = 7.0$ Hz, 4H; CH_2NH_2), 2.70 (m, 6H; NCH_2), 1.67 (m, $J = 7.2$ Hz, 4H; $NCH_2CH_2CH_2N$), 1.53–1.35 (m, 8H; $CH_2CH_2CH_2CH_2$), 1.47 ppm (s, 9H; CH_3); ^{13}C NMR (CD_3OD): $\delta = 121.3$, 80.1, 55.3, 53.2, 41.6, 41.4, 31.3, 30.7, 29.1, 28.7, 28.1, 27.8 ppm; MS (FAB): m/z calcd for $[M+H]^+$: 331.3; found: 331.3.

6: The same procedure as for wedge **4** was used, starting from diamine wedge **5** (0.28 g, 0.85 mmol) and acrylonitrile (0.28 mL, 4.24 mmol) in water (5 mL), to give **6** as a yellow oil (0.45 g, 0.84 mmol; 98%). ^{1}H NMR ($CDCl_3$): $\delta = 4.52$ (s, 1H; NH), 3.08 (q, $J = 6.7$ Hz, 2H; $NHCH_2$), 2.83 (t, $J = 6.6$ Hz, 8H; CH_2CN), 2.55 (t, $J = 7.1$ Hz, 4H; $NCH_2CH_2CH_2N$), 2.46 (m, 12H; NCH_2), 2.36 (t, $J = 7.1$ Hz, 2H; NCH_2), 1.57 (m, $J = 7.0$ Hz, 4H; $NCH_2CH_2CH_2N$), 1.48–1.22 (m, 8H; $CH_2CH_2CH_2CH_2$), 1.42 ppm (s, 9H; CH_3); ^{13}C NMR ($CDCl_3$): $\delta = 155.6$, 118.3, 78.5, 53.5, 51.2, 51.0, 49.2, 40.1, 29.6, 28.0, 26.8, 26.5, 26.3, 24.7, 16.5 ppm; MS (MALDI-TOF): m/z calcd for $[M+H]^+$: 543.4; found: 543.5.

7: The same procedure as for wedge **5** was used, starting from tetranitrile wedge **6** (0.45 g, 0.84 mmol), to give **7** as a yellow oil (0.46 g, 0.82 mmol; 97%). ^{1}H NMR (CD_3OD): $\delta = 3.07$ (t, $J = 7.0$ Hz, 2H; $NHCH_2$), 2.72 (t, $J = 7.1$ Hz, 8H; CH_2NH_2), 2.67–2.48 (m, 18H; NCH_2), 1.68 (m, $J = 7.2$ Hz, 12H; $NCH_2CH_2CH_2N$), 1.51–1.36 (m, 8H; $CH_2CH_2CH_2CH_2$), 1.47 ppm (s, 9H; CH_3); ^{13}C NMR (CD_3OD): $\delta = 158.4$, 80.1, 55.3, 53.5, 53.1, 41.6, 41.4, 31.3, 30.7, 29.1, 28.7, 28.2, 27.8, 25.0, 24.8 ppm; MS (MALDI-TOF): m/z calcd for $[M+H]^+$: 559.5; found: 559.9.

8: 1-Adamantyl isocyanate (0.64 g, 3.62 mmol) was added to a solution of tetraamine wedge **7** (0.46 g, 0.82 mmol) in chloroform (10 mL). The mixture was stirred overnight at room temperature under argon. The solvent was removed under reduced pressure, then diethyl ether was added, and the formed precipitate was isolated and dried under reduced pressure to give **8** as a white solid (0.85 g, 0.67 mmol; 82%). ^{1}H NMR ($CDCl_3$): $\delta = 5.72$ (s, 4H; $CH_2NHCONH$), 5.06 (s, 4H; NHCONHAd), 4.66 (s, 1H; NHCO), 3.09 (m, 10H; $NHCH_2$), 2.38 (m, 18H; NCH_2), 2.03 (s, 12H; CH), 1.96 (s, 24H; $NHCCH_2$), 1.64 (s, 24H; $CHCH_2CH$), 1.58 (m, 12H; $NCH_2CH_2CH_2N$), 1.43 (s, 9H; CH_3), 1.46–1.24 ppm (m, 8H; $NCH_2CH_2CH_2CH_2CH_2CH_2$); ^{13}C NMR ($CDCl_3$): $\delta = 158.4$, 156.2, 52.1, 51.7, 51.6, 50.6, 42.6, 38.3, 36.5, 30.9, 30.1, 29.6, 28.4, 27.9, 26.8, 26.6 ppm; MS (MALDI-TOF): m/z calcd for $[M+H]^+$: 1268.0, found: 1268.6.

9: To a cooled solution of **8** (201 mg, 0.16 mmol) in CH_2Cl_2 (10 mL) was added trifluoroacetic acid (0.5 mL). The solution was stirred for 30 min, after which time the solvent was evaporated. The excess trifluoracetic acid was removed azeotropically with toluene. The residue was triturated with diethyl ether to give **9** as a white solid (177 mg, 0.15 mmol; 95%). ^{1}H NMR ($CDCl_3$): $\delta = 3.24$–2.83 (m, 30H; $NHCH_2 + NCH_2 + CH_2NH_2$), 1.97 (s, 12H; CH), 1.86 (s, 24H; $NHCCH_2$), 1.78 (m, 12H; $NCH_2CH_2CH_2N$), 1.58 (s, 24H; $CHCH_2CH$), 1.40–1.21 ppm (m, 8H; $NCH_2CH_2CH_2CH_2CH_2$); ^{13}C NMR ($CDCl_3$): $\delta = 158.7$, 52.6, 50.4, 49.3, 42.6, 41.7, 39.6, 35.9, 30.7, 30.0, 29.1, 28.9, 27.9, 25.6, 25.5, 24.2 ppm; MS (MALDI-TOF): m/z calcd for $[M+Na]^+$: 1189.9; found: 1190.2.

1: To a solution of adamantyl-terminated dendritic wedge **8** (93 mg, 0.080 mmol) and *N*,*N*-diisopropylethylamine (DIPEA; 40 µL, 0.24 mmol) in CH_2Cl_2 (20 mL) was added lissamine sulfonyl chloride (mixed isomers, 46 mg, 0.24 mmol). The solution was stirred overnight at room temperature. The solvent was evaporated under reduced pressure, and the residue was purified by gradient column chromatography (CH_2Cl_2/MeOH/Et_3N = 97.5:2:0.5 to 89.5:10:0.5) to give the desired product as a purple solid (53 mg, 0.031 mmol; 37% yield). ^{1}H NMR ($CDCl_3$): $\delta = 8.67$ (s, 1H; ArH), 8.02 (d, $J = 7.7$ Hz, 1H; ArH), 7.17–7.13 (m, 3H; ArH), 6.79 (d, $J = 9.3$ Hz, 2H; ArH), 6.64 (s, 2H; ArH), 6.26 (s, 1H; ArH), 6.01–5.75 (m, 5H; $NHSO_2 + CH_2NHCO$), 5.38–5.08 (brs, 4H; AdNHCO), 3.56 (q, $J = 7.3$ Hz, 8H; $ArNCH_2CH_3$), 3.27 (q, $J = 7.3$ Hz, 2H; CH_2NHSO_2), 3.01 (bs, 8H; $CH_2NHCONH$), 2.58–2.19 (m, 18H; CH_2NCH_2), 1.91 (brs, 12H; AdH), 1.84 (brs, 24H; AdH), 1.61–1.40 (m, 36H; $AdH + NCH_2CH_2CH_2N + NCH_2CH_2CH_2NHCO$), 1.35–1.02 ppm (m, 20H; $CH_3CH_2 + NCH_2CH_2CH_2CH_2CH_2CH_2NSO_2$); ^{13}C NMR ($CDCl_3$): $\delta = 159.5$, 158.6, 157.9 155.6, 146.8, 143.1, 139.3, 133.5, 133.3, 129.1, 127.9, 127.3, 95.8, 52.4, 51.6, 51.4, 50.7, 46.0, 44.4, 42.5, 37.8, 36.6, 31.4, 29.6, 29.4–26.4, 22.7, 12.6 ppm; MS (MALDI-TOF): m/z calcd for $[M+Na]^+$: 1731.1; found: 1731.2.

10: A solution of 1-bromoadamantane (15.0 g, 69.8 mmol) and triethylamine (30 mL, 216 mmol) in tetraethylene glycol (250 mL) was stirred overnight at 180 °C. After cooling to room temperature, dichloromethane (250 mL) was added. The solution was washed with 2 M hydrochloric acid (4 × 100 mL) and once with brine (100 mL). The organic layer was dried over $MgSO_4$ and the solvent was evaporated under reduced pressure to give **10** as a yellow-brown oil (21.8 g, 66.4 mmol; 95%). ^{1}H NMR ($CDCl_3$): $\delta = 3.73$ (t, $J = 4.6$ Hz, 2H; $AdOCH_2CH_2$), 3.69–3.66 (m, 8H; OCH_2CH_2O), 3.64–3.58 (m, 6H; $AdOCH_2CH_2 + CH_2CH_2OH$), 2.89 (s, 1H; CH_2OH), 2.15 (m, 3H; CH_2CHCH_2[Ad]), 1.75–1.76 (m, 6H; $CHCH_2$C[Ad]), 1.67–1.57 ppm (m, 6H; $CHCH_2$CH[Ad]); ^{13}C NMR ($CDCl_3$): $\delta = 72.0$, 71.8, 70.8, 70.1, 70.0, 69.8, 61.2, 58.7, 40.9, 35.9, 30.0 ppm; MS (FAB): m/z calcd for $[M+H]^+$: 329.3; found: 329.3.

11: A solution of phosphorus tribromide (1.30 g, 4.80 mmol) in toluene (50 mL) was added dropwise to a cooled (0 °C) solution of **10** (4.03 g, 12.2 mmol) in toluene (100 mL). The mixture was stirred overnight at room temperature. The solvent was removed under reduced pressure and the residue was partitioned between dichloromethane (100 mL) and water (100 mL). The organic layer was washed with water (3 × 50 mL) and brine (1 × 50 mL) and dried over $MgSO_4$. The solvent was removed under reduced pressure and the residue was purified by column chromatography (CH_2Cl_2/MeOH = 99:1) to give **11** as a colorless oil (2.48 g, 6.4 mmol; 52%). ^{1}H NMR ($CDCl_3$): $\delta = 3.83$ (t, $J = 6.2$ Hz, 2H; $AdOCH_2CH_2$), 3.70–3.67 (m, 8H; OCH_2CH_2O), 3.62–3.60 (m, 4H; $AdOCH_2CH_2 + CH_2CH_2Br$), 3.49 (t, $J = 6.4$ Hz, 2H; CH_2CH_2Br), 2.15 (m, 3H; CH_2CHCH_2[Ad]), 1.76–1.75 (m, 6H; $CHCH_2$C[Ad]), 1.64–1.62 ppm (m, 6H; $CHCH_2$CH[Ad]); ^{13}C NMR ($CDCl_3$): $\delta = 72.2$, 71.3, 71.2, 70.7–70.5, 59.2, 41.4, 36.4, 30.4 ppm; MS (FAB): m/z calcd for $[M+H]^+$: 391.1; found: 391.2.

12: A suspension of **11** (1.68 g, 4.29 mmol), 3,5-dihydroxybenzonitrile (0.28 g, 2.04 mmol), dried potassium carbonate (0.71 g, 5.14 mmol), and [18]crown-6 (0.11 g, 0.42 mmol) in acetone (50 mL) was refluxed for 72 h. The solvent was evaporated and the residue was partitioned between water (50 mL) and diethyl ether (50 mL). The aqueous layer was extracted with diethyl ether (3 × 25 mL) and the combined extracts were dried over $MgSO_4$. The solvent was evaporated and the residue was purified by column chromatography (CH_2Cl_2/MeOH = 98:2) to give **12** as a colorless oil (0.54 g, 0.72 mmol; 35 %). ^{1}H NMR ($CDCl_3$): δ = 6.80 (d, J = 2.2 Hz, 2H, ArH), 6.73 (t, J = 2.2 Hz, 1H; ArH]), 4.13 (t, J = 4.8 Hz, 4H; $ArOCH_2$), 3.87 (t, J = 4.8 Hz, 4H; $AdOCH_2$), 3.76–3.67 (m, 16H; OCH_2CH_2O), 3.63–3.58 (m, 8H; $AdOCH_2CH_2$ + CH_2CH_2OAr), 2.15 (m, 3H; CH_2CHCH_2[Ad]), 1.75–1.76 (m, 6H; $CHCH_2C$[Ad]), 1.68–1.58 ppm (m, 6H; $CHCH_2CH$[Ad]); ^{13}C NMR ($CDCl_3$): δ = 160.1, 118.7, 113.3, 110.7, 106.7, 72.3, 71.3, 70.9, 70.6–70.5, 69.4, 67.9, 59.2, 41.4, 36.4, 30.5 ppm; MS (FAB): m/z calcd for $[M+H]^+$: 756.5; found: 756.3.

13: Compound **12** (0.54 g, 0.71 mmol) was dissolved in 6 M ammonia in ethanol (50 mL) and some Raney cobalt was added. The mixture was placed in an autoclave and stirred overnight under 5 bar H_2 at room temperature. The suspension was filtered over celite and washed with methanol (1 L). The solvent was evaporated under reduced pressure and the residue was dissolved in chloroform (50 mL). The solution was washed with a 0.1 M NaOH solution, the organic layer was separated, and the aqueous layer was extracted with chloroform (3 × 200 mL). The solvent of the combined organic fractions was evaporated under reduced pressure to give **13** as a colorless oil (0.50 g, 0.66 mmol; 92 %). ^{1}H NMR ($CDCl_3$): δ = 6.55 (s, 2H; ArH), 6.39 (s, 1H; ArH), 4.13 (t, J = 4.8 Hz; 4H, $ArOCH_2$), 3.86 (m, 6H; $AdOCH_2$ + CH_2NH_2), 3.76–3.65 (m, 18H; OCH_2CH_2O + CCH_2NH_2), 3.60 (m, 8H; $AdOCH_2CH_2$ + CH_2CH_2OAr), 2.16 (m, 6H; CH_2CHCH_2[Ad]), 1.75–1.76 (m, 12H; $CHCH_2C$[Ad]), 1.68–1.58 ppm (m, 12H; $CHCH_2CH$[Ad]); ^{13}C NMR ($CDCl_3$): δ = 160.0, 106.3, 100.3, 72.4, 71.2, 70.7–70.5, 69.8, 67.4, 65.0, 59.2, 41.4, 36.4, 30.5 ppm; MS (FAB): m/z calcd for $[M+H]^+$: 760.5; found: 760.3.

2: A solution of **13** (290 mg, 0.38 mmol), fluorescein isothiocyanate (297 mg, 0.76 mmol), DIPEA (0.5 mL, 2.87 mmol) in an 4:1 methanol/dichloromethane mixture (50 mL) was stirred overnight at room temperature. The solvent was evaporated under reduced pressure and the residue was purified by gradient column chromatography (CH_2Cl_2/MeOH = 99:1 to 96:4) to give **2** as a yellow solid (80 mg, 0.070 mmol; 18 %). ^{1}H NMR ($CDCl_3$): δ = 10.25 (b, 1H; ArCOOH), 9.83 (s, 1H; ArOH), 8.36 (s, 1H, ArH), 8.05 (b, 1H; ArNHCS), 7.95 (d, J = 8.4 Hz, 1H; ArH), 6.98 (d, J = 8.4 Hz, 1H; ArH), 6.77 (s, 2H; ArH), 6.62–6.52 (m, 6H; ArH), 6.29 (s, 1H; ArH), 4.76 (s, 2H; $ArCH_2NH$), 4.01–3.95 (m, 5H; $ArOCH_2$ + CH_2NHCS), 3.75 (m, 4H; $AdOCH_2$), 3.66–3.56 (m, 24H; OCH_2CH_2O + $AdOCH_2CH_2$ + CH_2CH_2OAr), 2.10 (m, 6H; CH_2CHCH_2[Ad]), 1.71 (m, 12H; $CHCH_2C$[Ad]), 1.62–1.52 ppm (m, 12H; $CHCH_2CH$[Ad]); ^{13}C NMR ($CDCl_3$): δ = 181.2, 169.8, 159.8, 152.8, 141.4, 140.2, 130.5, 129.9, 129.1, 128.3, 127.5, 122.2, 118.1, 110.5, 108.0, 106.5, 103.1, 100.6, 72.7, 71.2, 70.5–70.4, 69.6, 67.3, 59.2, 54.0, 48.1, 42.2, 41.3, 36.3, 30.4 ppm; MS (FAB): m/z calcd for $[M+H]^+$: 1149.5; found: 1149.6.

3: A solution of **13** (210 mg, 0.28 mmol), lissamine sulfonyl chloride (mixture of isomers, 319 mg, 0.55 mmol), and DIPEA (0.5 mL, 2.87 mmol) in acetonitrile (50 mL) was stirred overnight at room temperature. The solvent was evaporated under reduced pressure and the residue was purified by gradient column chromatography (CH_2Cl_2/MeOH = 99:1 to 94:6) to give the single isomer **3** as a purple solid (92 mg, 0.071 mmol; 26 %). ^{1}H NMR ($CDCl_3$): δ = 8.85 (s, 1H; ArH), 7.90 (d, J = 9.5 Hz, 1H; ArH), 7.26 (d, J = 9.5 Hz, 2H; ArH), 7.13 (d, J = 8.1 Hz, 1H; ArH), 6.85 (d, J = 9.5 Hz, 2H; ArH), 6.67 (s, 2H; ArH), 6.52 (s, 2H; ArH), 6.34 (s, 1H; ArH), 6.16 (brs, 1H; CH_2NHS), 4.18 (d, J = 5.9 Hz, 2H; CCH_2NH), 4.08 (t, J = 4.6 Hz, 4H; $ArOCH_2$), 3.80 (t, J = 4.8 Hz, 4H; $AdOCH_2$), 3.72–3.62 (m, 16H, OCH_2CH_2O), 3.62–3.50 (m, 16H; $AdOCH_2CH_2$ + CH_2CH_2OAr + NCH_2CH_3), 2.13 (m, 6H; CH_2CHCH_2[Ad]), 1.74 (m, 12H; $CHCH_2C$[Ad]), 1.66–1.56 (m, 12H; $CHCH_2CH$[Ad]), 1.31 ppm (t, J = 7.1 Hz, 12H; NCH_2CH_3); ^{13}C NMR ($CDCl_3$): δ = 159.8, 158.9, 157.8, 155.4, 147.8, 142.1, 139.2, 133.6, 133.4, 129.5, 127.3, 127.0, 114.3, 113.5, 106.4, 101.5, 95.5, 72.2, 71.1, 70.6–70.5, 69.6, 67.4, 59.2, 47.3, 45.8, 41.4, 36.4, 30.4, 12.6 ppm. MS (MALDI-TOF): m/z calcd for $[M+H]^+$: 1300.6; found: 1300.4.

Microcontact printing: Stamps were prepared by casting a 10:1 (v/v) mixture of poly(dimethylsiloxane) and curing agent (Sylgard 184, Dow Corning) against a silicon master. After overnight curing at 60 °C, the stamps were mildly oxidized in an UV/ozone reactor for 30–60 min and subsequently inked by soaking them into an aqueous adsorbate solution for at least 5 min. Before printing, the stamps were blown dry in a stream of N_2. The stamps were brought into conformal contact with the substrate by hand, without the use of external pressure. Printing on the preformed monolayers was performed for 60 s, after which time the stamp was carefully removed. After each printing step the inking procedure was repeated. Microcontact-printed substrates were imaged directly after printing, or after thorough rinsing with 200 mL of aqueous solutions of phosphate buffer (10 mM, pH 7), NaCl (50 mM), or native CD (10 mM).

Dip-pen nanolithography: Glass microscope slides were hand-marked using a diamond tip prior to monolayer preparation. Before the writing procedure was carried out, the marked substrates were bleached extensively to reduce background fluorescence. For bleaching, the substrates were exposed to the 435 and 546 nm lines of a mercury lamp with a power of approximately 900 mW. The light was focused on the marker using an oil immersion lens (N.A. 1.4, 63 ×). The exposure time was at least 30 min per line.

For the DPN experiments, Si_3N_4 tips coated with 50 nm of gold were used (Ssens BV, The Netherlands). To reduce the activation energy required for molecular transport from tip to surface, gold-coated Si_3N_4 tips were covered with an oligo(ethylene glycol) SAM.[21] Cleaned gold tips were immersed in a 0.1 mM solution of a thiolated oligo(ethylene glycol) derivative in ethanol overnight, subsequently rinsed with ethanol, and dried in a stream of nitrogen. For the writing experiments the tips were inked by soaking them in a 0.1 mM ethanol solution of **3** or 10 μM aqueous solution of the per-CD complex of **1** for 5 min and dried in air. The tips were mounted in the AFM head, and the AFM cantilever was positioned within the marker with the use of a CCD camera. Patterns were written in the vicinity of the marker.

AFM: AFM experiments were carried out with a Nanoscope IIIa multimode AFM (Digital Instruments, Santa Barbara, CA, USA) in contact mode using V-shaped Si_3N_4 cantilevers (Nanoprobes, Digital Instruments). For imaging, cantilevers with a spring constant of 0.1 $N\,m^{-1}$ were used. Images were acquired in ambient atmosphere ($\approx$30–40% relative humidity, 25 °C). For writing purposes, gold-coated tips with a spring constant of 0.58 $N\,m^{-1}$ were used. Writing experiments were conducted at increased relative humidity and temperature ($\approx$50% relative humidity, 29 °C). The cross in Figure 8 was written by scanning each 10 μm line for 10 min at a scan rate of 20 $\mu m\,s^{-1}$, and with an aspect ratio of 64:1. The eight-pointed star in Figure 9 was written by scanning each 15 μm line 10 times at a scan rate of 22.5 $\mu m\,s^{-1}$, and with an aspect ratio of 32:1. The load used during writing experiments was generally $\leq$15 nN.

Laser scanning confocal microscopy: Confocal microscopy images of the microcontact-printed substrates were taken on a Carl Zeiss LSM 510 microscope. The light was focused on the substrate using an oil immersion lens (N.A. 1.4, 63×). The lissamine-functionalized wedges were excited at 543 nm, while the fluorescein-functionalized wedge was excited at 488 nm. The emitted fluorescence was collected on a PMT R6357 spectrophotometer. All confocal microscopy images were acquired in air.

Fluorescence imaging of the DPN patterns was carried out on a set-up suited for single-molecule imaging,[54] using an inverted confocal microscope (Zeiss Axiovert) with an oil immersion lens (N.A. 1.4, 100×). An ArKr ion laser (Spectra Physics Beamlok 2060) operated at 514 nm was used to excite the fluorophores. The excitation light was filtered using a 514 bandpass filter (Omega 514.5/10). A dichroic mirror (Omega 540DRLP) and a long-pass filter (Omega 550APL) were used to separate the emitted light from the excitation light. The fluorescence signal was detected using an avalanche photodiode (EG&G Electro Optics SPCM-AQ-14). The sample was scanned over an area, typical 30×30 μm with 512×512 pixels and a pixel dwell time of 1 ms. The excitation power was $\approx$3.5 $kW\,cm^{-2}$. All confocal microscope images were acquired in air.

[1] F. Arias, L. A. Godinez, S. R. Wilson, A. E. Kaifer, L. Echegoyen, *J. Am. Chem. Soc.* **1996**, *118*, 6086–6087.

[2] Y. Miura, S. Kimura, Y. Imanishi, J. Umemura, *Langmuir* **1998**, *14*, 2761–2767.

[3] A. Fragoso, J. Caballero, E. Almirall, R. Villalonga, R. Cao, *Langmuir* **2002**, *18*, 5051–5054.

[4] J. Huskens, M. A. Deij, D. N. Reinhoudt, *Angew. Chem.* **2002**, *114*, 4647–4651; *Angew. Chem. Int. Ed.* **2002**, *41*, 4467–4471.

[5] I. A. Banerjee, L. T. Yu, H. Matsui, *J. Am. Chem. Soc.* **2003**, *125*, 9542–9543.

[6] A. Sanyal, T. B. Norsten, O. Uzun, V. M. Rotello, *Langmuir* **2004**, *20*, 5958–5964.

[7] M. Mammen, S.-K. Choi, G. M. Whitesides, *Angew. Chem.* **1998**, *110*, 2908–2953; *Angew. Chem. Int. Ed.* **1998**, *37*, 2754–2794.

[8] C. Dietrich, L. Schmitt, R. Tampé, *Proc. Natl. Acad. Sci. U.S.A.* **1995**, *92*, 9014–9018.

[9] A. Thess, S. Hutschenreiter, M. Hofmann, R. Tampé, W. Baumeister, R. Guckenberger, *J. Biol. Chem.* **2002**, *277*, 36321–36328.

[10] S. J. Metallo, R. S. Kane, R. E. Holmlin, G. M. Whitesides, *J. Am. Chem. Soc.* **2003**, *125*, 4534–4540.

[11] J. Huskens, A. Mulder, T. Auletta, C. A. Nijhuis, M. J. W. Ludden, D. N. Reinhoudt, *J. Am. Chem. Soc.* **2004**, *126*, 6784–6797.

[12] M. W. J. Beulen, J. Bügler, B. Lammerink, F. A. J. Geurts, E. M. E. F. Biemond, K. G. C. van Leerdam, F. C. J. M. van Veggel, J. F. J. Engbersen, D. N. Reinhoudt, *Langmuir* **1998**, *14*, 6424–6429.

[13] H. Schönherr, M. W. J. Beulen, J. Bügler, J. Huskens, F. C. J. M. van Veggel, D. N. Reinhoudt, G. J. Vancso, *J. Am. Chem. Soc.* **2000**, *122*, 4963–4967.

[14] M. Rekharsky, Y. Inoue, *Chem. Rev.* **1998**, *98*, 1875–1917.

[15] M. W. J. Beulen, J. Bügler, M. R. de Jong, B. Lammerink, J. Huskens, H. Schönherr, G. J. Vancso, B. A. Boukamp, H. Wieder, A. Offenhäuser, W. Knoll, F. C. J. M. van Veggel, D. N. Reinhoudt, *Chem. Eur. J.* **2000**, *6*, 1176–1183.

[16] M. R. de Jong, J. Huskens, D. N. Reinhoudt, *Chem. Eur. J.* **2001**, *7*, 4164–4170.

[17] T. Auletta, M. R. de Jong, A. Mulder, S. Zapotoczny, S. Zou, H. Schönherr, J. Huskens, F. C. J. M. van Veggel, D. N. Reinhoudt, G. J. Vancso, *J. Am. Chem. Soc.* **2004**, *126*, 1577–1584.

[18] A. Mulder, T. Auletta, A. Sartori, S. Del Ciotto, A. Casnati, R. Ungaro, J. Huskens, D. N. Reinhoudt, *J. Am. Chem. Soc.* **2004**, *126*, 6627–6636.

[19] T. Auletta, B. Dordi, A. Mulder, A. Sartori, S. Onclin, C. M. Bruinink, M. Péter, C. A. Nijhuis, H. Beijleveld, H. Schönherr, G. J. Vancso, A. Casnati, R. Ungaro, B. J. Ravoo, J. Huskens, D. N. Reinhoudt, *Angew. Chem.* **2004**, *116*, 373–377; *Angew. Chem. Int. Ed.* **2004**, *43*, 369–373.

[20] S. Onclin, A. Mulder, J. Huskens, B. J. Ravoo, D. N. Reinhoudt, *Langmuir* **2004**, *20*, 5460–5466.

[21] R. Singhvi, A. Kumar, G. P. Lopez, G. N. Stephanopoulos, D. I. C. Wang, G. M. Whitesides, D. E. Ingber, *Science* **1994**, *264*, 696–698.

[22] P. C. Hidber, W. Helbig, E. Kim, G. M. Whitesides, *Langmuir* **1996**, *12*, 1375–1380.

[23] J. H. Lim, D. S. Ginger, K. B. Lee, J. Heo, J. M. Nam, C. A. Mirkin, *Angew. Chem.* **2003**, *115*, 2411–2414; *Angew. Chem. Int. Ed.* **2003**, *42*, 2309–2312.

[24] T. P. Sullivan, W. T. S. Huck, *Eur. J. Org. Chem.* **2003**, 17–29.

[25] Y. N. Xia, G. M. Whitesides, *Angew. Chem.* **1998**, *110*, 568–594; *Angew. Chem. Int. Ed.* **1998**, *37*, 551–575.

[26] D. S. Ginger, H. Zhang, C. A. Mirkin, *Angew. Chem.* **2004**, *116*, 30–46; *Angew. Chem. Int. Ed.* **2004**, *43*, 30–45.

[27] The excited state of fluorescent molecules situated at or near the gold surface couples with the surface plasmons of the gold, which results in energy transfer from the fluorescent dye to the surface without emission of light. This quenching process is a well-known phenomenon for fluorescent molecules near metallic interfaces, and for this reason fluorescence imaging is typically limited to oxide surfaces, for example, silicon oxide. See: a) R. Chance, A. Prock, R. Silbey, *Adv. Chem. Phys.* **1978**, *37*, 1–65; b) J. Enderlein, *Chem. Phys.* **1999**, *247*, 1–9; c) J. Kümmerlen, A. Leitner, H. Brunner, F. R. Aussenegg, A. Wokaun, *Mol. Phys.* **1993**, *80*, 1031–1046; d) S. Reese, M. A. Fox, *J. Phys. Chem. B* **1998**, *102*, 9820–9824.

[28] Quenching especially hampers fluorescence spectroscopy at continuous metallic films, but is less predominant at metallic nanoparticles or islands, see for example Ref. [30] and: a) S. A. Levi, A. Mourran, J. P. Spatz, F. C. J. M. van Veggel, D. N. Reinhoudt, M. Möller, *Chem. Eur. J.* **2002**, *8*, 3808–3814; b) E. Dulkeith, A. C. Morteani, T. Niedereichholz, T. A. Klar, J. Feldmann, S. A. Levi, F. C. J. M. van Veggel, D. N. Reinhoudt, M. Möller, D. I. Gittins, *Phys. Rev. Lett.* **2002**, *89*, Art. No. 203002, 1–3; c) G. Chumanov, K. Sokolov, B. W. Gregory, T. M. Cotton, *J. Phys. Chem.* **1995**, *99*, 9466–9471.

[29] S. Weiss, *Science* **1999**, *283*, 1676–1683.

[30] V. C. H. Chan, S. L. Codd, M. van der Helm, J. P. Spatz, C. Röcker, G. U. Nienhaus, S. A. Levi, F. C. J. M. van Veggel, D. N. Reinhoudt, M. Möller, *J. Mater. Res.* **2001**, *16*, Y4.4.

[31] T. Yang, O. K. Baryshikova, H. Mao, M. A. Holden, P. S. Cremer, *J. Am. Chem. Soc.* **2003**, *125*, 4779 – 4784.

[32] To make differentiation between different molecules by AFM feasible, the probed molecules should display substantially different wetting properties, see for example: S. Hong, C. A. Mirkin, *Science* **2000**, *288*, 1808 – 1811; b) S. Hong, J. Zhu, C. A. Mirkin, *Science* **1999**, *286*, 523 – 525.

[33] C. Pale-Grosdemange, E. S. Simon, K. L. Prime, G. M. Whitesides, *J. Am. Chem. Soc.* **1991**, *113*, 12 – 20.

[34] S. W. Lee, P. E. Laibinis, *Biomaterials* **1998**, *19*, 1669 – 1675.

[35] A. Papra, N. Gadegaard, N. B. Larsen, *Langmuir* **2001**, *17*, 1457 – 1460.

[36] F. Corbellini, A. Mulder, A. Sartori, M. Ludden, A. Casnati, R. Ungaro, J. Huskens, M. Crego-Calama, D. N. Reinhoudt, *J. Am. Chem. Soc.* **2004**, *126*, in press.

[37] a) J. A. Bell, C. Kenworthy, *Synthesis* **1971**, 650 – 652; b) E. M. M. de Brabander-van den Berg, E. W. Meijer, *Angew. Chem.* **1993**, *105*, 1370 – 1372; *Angew. Chem. Int. Ed. Engl.* **1993**, *32*, 1308 – 1311; c) E. M. M. de Brabander, J. Brackman, M. Mure-Mak, H. de Man, M. Hogeweg, J. Keulen, R. Scherrenberg, B. Coussens, Y. Mengerink, S. van der Wal, *Macromol. Symp.* **1996**, *102*, 9 – 17.

[38] C. J. Hawker, J. M. J. Fréchet, *J. Am. Chem. Soc.* **1990**, *112*, 7638 – 7647.

[39] Wedges bearing more adamantyl moieties are readily accessible by using 3,5-dihydroxybenzyl alcohol instead of 3,5-dihydroxybenzonitrile. This procedure can be repeated to obtain wedges bearing up to 32 adamantyl groups. However, these larger molecules have poor water solubility, even in the presence of CD (see K. J. C. van Bommel, G. A. Metselaar, W. Verboom, D. N. Reinhoudt, *J. Org. Chem.* **2001**, *66*, 5405 – 5412). For this reason the synthesis was limited to the bis(adamantyl)-functionalized fluorescent molecules **2** and **3**.

[40] A tetravalent interaction between **1** and the CD monolayer leads to complex stabilities that give rise to patterns that show no detectable desorption after rinsing with 10 mM CD, see Refs. [4], [11], and [36].

[41] C. A. Nijhuis, J. Huskens, D. N. Reinhoudt, *J. Am. Chem. Soc.* **2004**, *126*, 12 266 – 12 267.

[42] J. L. Wilbur, A. Kumar, E. Kim, G. M. Whitesides, *Adv. Mater.* **1994**, *6*, 600 – 604.

[43] N. B. Larsen, H. Biebuyck, E. Delamarche, B. Michel, *J. Am. Chem. Soc.* **1997**, *119*, 3017 – 3026.

[44] N. L. Jeon, K. Finnie, K. Branshaw, R. G. Nuzzo, *Langmuir* **1997**, *13*, 3382 – 3391.

[45] L. B. Goetting, T. Deng, G. M. Whitesides, *Langmuir* **1999**, *15*, 1182 – 1191.

[46] D. Arrington, M. Curry, S. C. Street, *Langmuir* **2002**, *18*, 7788 – 7791.

[47] The theoretical model developed by us for multivalent interactions at CD monolayers (Ref. [11]) and SPR experiments with other guest molecules having two adamantyl moieties (Ref. [18]) indicated that full saturation of the CD cavities at the monolayers is achieved when applying micromolar solutions of guests having two adamantyl moieties, and that there is no substantial removal of guest molecules from the monolayer when rinsed with water.

[48] M. V. Rekharsky, Y. Inoue, *Chem. Rev.* **1998**, *98*, 1875 – 1917.

[49] J. H. Lim, D. S. Ginger, K. B. Lee, J. Heo, J. M. Nam, C. A. Mirkin, *Angew. Chem.* **2003**, *115*, 2411 – 2414; *Angew. Chem. Int. Ed.* **2003**, *42*, 2309 – 2312.

[50] C. Pale-Grosdemange, S. E. Simon, K. L. Prime, G. M. Whitesides, *J. Am. Chem. Soc.* **1991**, *113*, 12 – 20.

[51] L. M. Demers, D. S. Ginger, S.-J. Park, Z. Li, S.-W. Chung, C. A. Mirkin, *Science* **2002**, *296*, 1836 – 1838.

[52] A CD-terminated glass slide was scanned with a bare Si_3N_4 tip under similar experimental conditions. Subsequent LFM imaging did not show any visible pattern, which indicates that the writing process did not damage the monolayer.

[53] D. D. Perrin, W. F. L. Armarego, *Purification of Laboratory Chemicals*, *3rd ed.*, Pergamon, Oxford, **1989**.

[54] J. Hernando, M. van der Schaaf, E. M. H. P. van Dijk, M. Sauer, M. F. García-Parajó, N. F. van Hulst, *J. Phys. Chem. A* **2003**, *107*, 43 – 52.

Received: August 25, 2004

